

## 7. Validation of the FE Model of IRJ

### 7.1. Introduction

The FE results are compared with the strain gauged experimental data in this chapter. Both the static and the dynamic FE analyses results are validated using the lab and field tests respectively. The comparison has generally been regarded as satisfactory.

The experiment is conducted as part of an ongoing research project at the Centre for Railway Engineering (CRE) with the support from QR. This thesis takes the advantage of the experiment by collecting limited experimental data for FE model validation. The vertical strain is selected for the result comparison.

### 7.2. Validation of Static FEA Model

The IRJ was supported in the lab test different to the condition in the field; hence, the boundary condition of the static FE model was modified. The results of the modified FE model are validated with the lab test data.

As introduced in the Chapter 6, in the static test the IRJ bottom was supported on two steel bars allowing free movement of the IRJ in the longitudinal direction. Referring to Fig. 7.1, for simplicity, the effect of the steel bar contact surface width (18mm) was modelled through coupling the rail bottom to the support bar via a reference node. The boundary condition of the reference nodes' DOF 3 was set free and the remaining

five DOFs were arrested. The beam element was also removed from the FE model as the IRJ section was only 2.4m long in the lab test. The boundary condition of the wheel was kept the same as described in Chapter 4 in which DOF 2 was set free and DOFs1 and 3 were arrested. The 150kN vertical load was applied to the railhead.

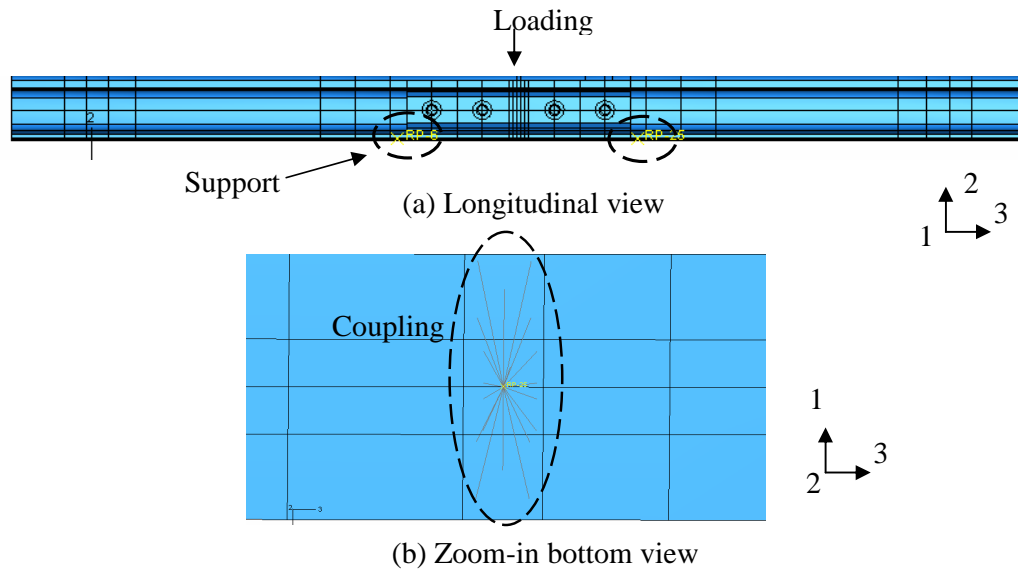


Figure 7.1 Support system of static test

Six different loading positions were simulated in the static FE model. The positions of strain gauges and loadings are illustrated in Fig. 7.2.

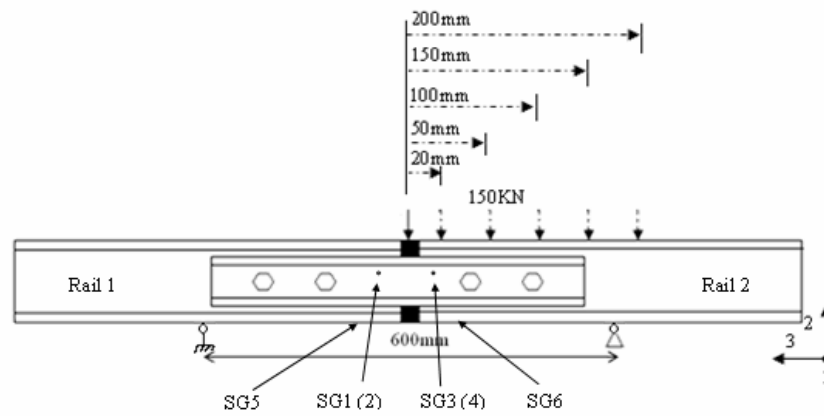


Figure 7.2 Positions of strain gauges and loadings

In Figs. 7.3 and 7.4, the horizontal axis represents the loading positions and the vertical axis shows the vertical strain magnitude. Fig 7.3 shows that the FE results agree well with the tests for the Strain Gauge 1/2. The maximum difference appears at the loading position at the centre (0mm) where the result of the lab test is 264.9 microstrain, while the FE model gave a magnitude of 258.1 with the difference being 2.57%  $((264.9-258.1)/264.9)$ . As the loading position moves, the  $E_{22}$  strain value from SG 1/2 decreases sharply to a low level. This is because at the 0mm loading position, half of static load is distributed to Rail 1; where the load is moved to other positions, the static load is concentrated on Rail 2. It is worth to note that in this thesis, for plotting convenience, the compression strain is regarded as positive and the tension strain is regarded as negative.

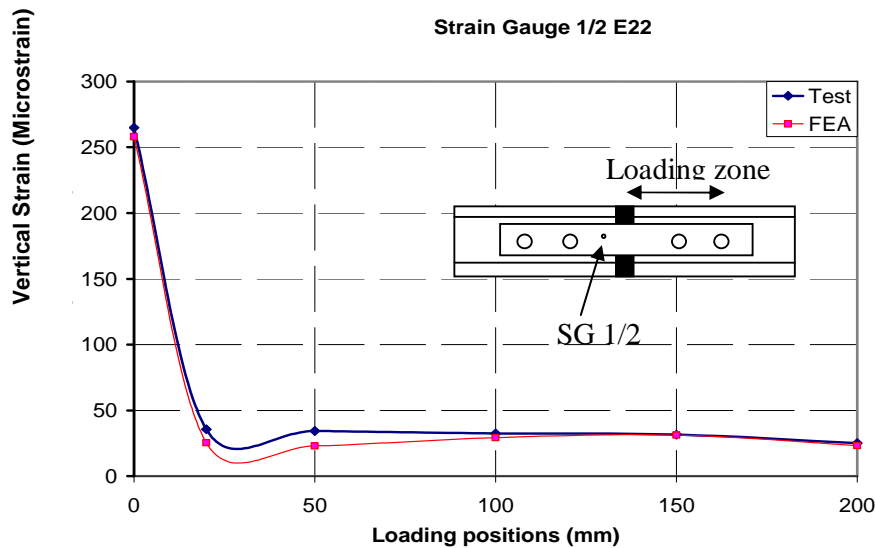


Figure 7.3 Vertical strain  $E_{22}$  comparison of Strain Gauge 1/2

The results from SG 3/4 exhibit a different trend as the loadings are positioned at both sides of the strain gauges. Referring to the Fig. 7.4, the peak value of  $E_{22}$  emerges at the 20mm loading position which is closest to the strain gauges (strain gauge 3/4 is

positioned at 20mm from the IRJ centre). At this point, the simulation error is 3.16% ((464.7-450.0)/464.7).

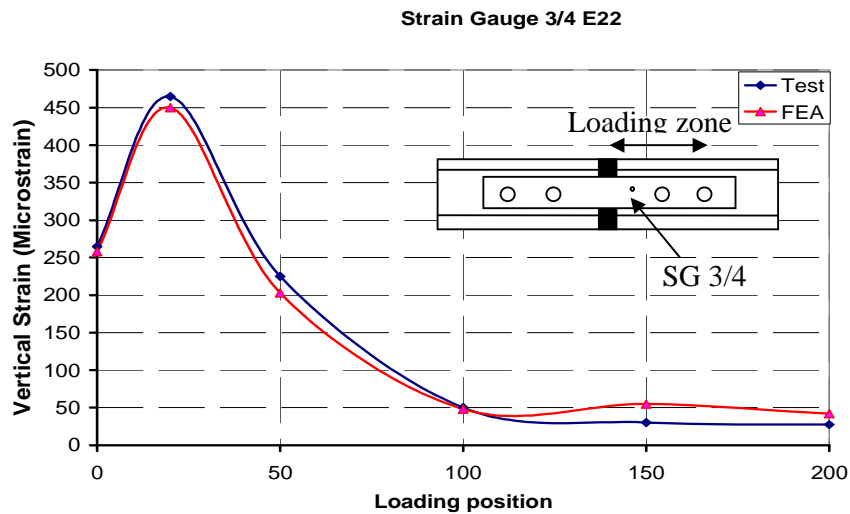


Figure 7.4 Vertical strain  $E_{22}$  comparison of Strain Gauge 3/4

### 7.3. Validation of Dynamic FEA Model

The major traffics on the rail route selected for the field test were the fully loaded heavy haul coal trains heading from left to right and coming back with empty wagons. In this section, two traffic conditions with different vertical wheel load, velocity and travel directions are investigated and compared with the dynamic FEA results.

Chapter 6 has provided brief details of how the traffic condition of the field test has been sorted out with the recorded strain time series. For the loaded coal wagons, the wheel travelling speed was approximately 74.5 Km/h and the vertical wheel load was 130.7 KN. This traffic condition was applied to the dynamic FE model and the strain time series of dynamic FEA were obtained. Because the strain gauges are on the Rail

2, referring to Fig. 7.5, the impact response between the wheel and the IRJ was captured by the strain gauges as explained in the previous chapter.

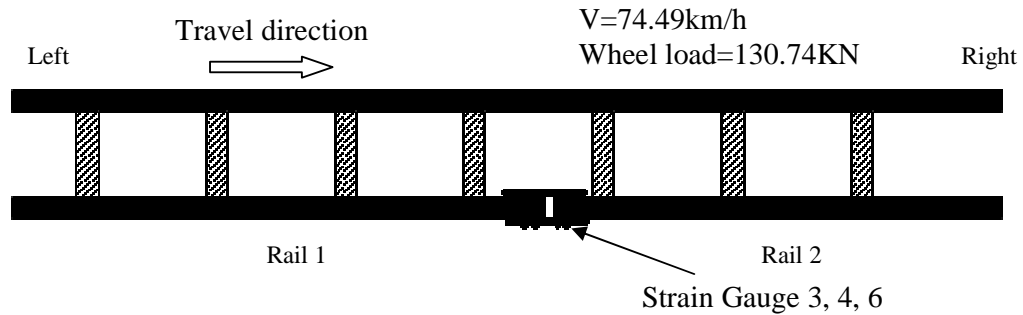


Figure 7.5 Illustrations of strain gauge location and travelling direction

There were 20 strain time series from 20 recorded wheel passages presented and compared to the FEA results. It is worth noting that the wheel loads were approximately close to 130.7KN calculated from the QR operational data which may lead to minor strain magnitude difference among these strain time series. The results of the comparison of vertical strain  $E_{22}$  is presented in Fig. 7.6. The vertical strain time series presents a satisfactory agreement between the field test and the FEA. The peak strain caused by the impact at the joint was an average 491.9 microstrain for the test and 469.3 microstrain for the FEA. The error is 4.69%  $((491.9-469.3)/491.9)$ . For the FE model, the second peak due to the location of strain gauges was not exhibited as prominently as in the field test data. The curves match well with similar curve slope and the steady strain value before impact.

In the other traffic condition, the empty train travels from right to left with a speed of 80.6 km/h and vertical wheel load of 28.91 KN, as shown in Fig. 7.7. In this condition,

the major impact occurs on the Rail 1; as only the strains in Rail 2 were monitored, the strains close to impact were not recorded. However strain peaks corresponding to wheel passage over strain gauge location was traceable. For the purpose of validating the dynamic FE model, such data was considered sufficient.

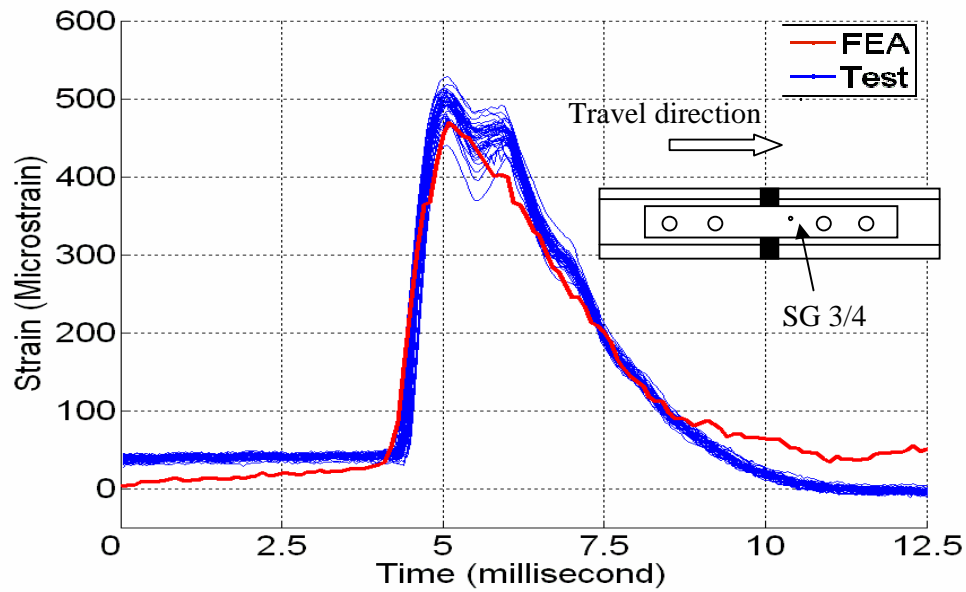


Figure 7.6 Vertical strain  $E_{22}$  comparison of Strain Gauge 3/4

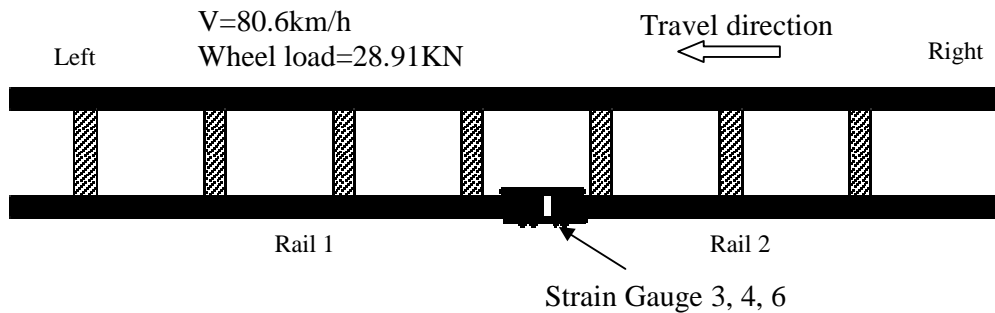


Figure 7.7 Illustrations of strain gauge location and travelling direction

Fig 7.8 presents that the peak values of FEA and field test are found relatively close. Before the peak, the FEA has predicted higher value of up to negative 60 microstrain. In the field test the strain were 10-20 microstrains at the beginning and gradually increases to 45 microstrain before the sharp surge to the peak.

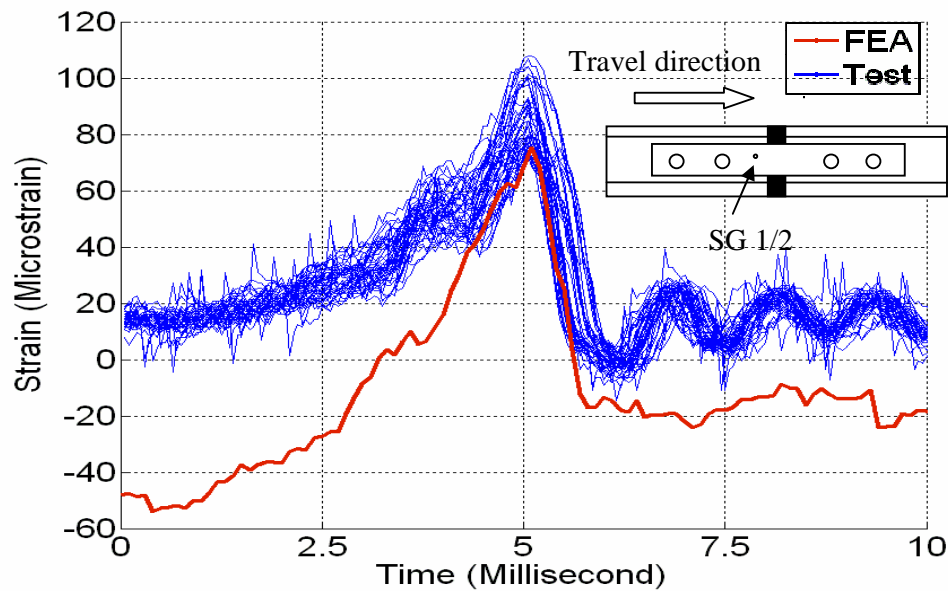


Figure 7.8 Vertical strain  $E_{22}$  comparison of Strain Gauge 3/4

#### 7.4. Summary

In this chapter the results of the tests and FE model were compared. The static results generally demonstrated satisfactory agreement between the lab test and static FE model. In the dynamic FE model validation section, two traffic conditions were investigated. Similar to the static analysis, the vertical strain on the rail web showed reasonable agreement between the FEA and test. In general, as the purpose of this research is to investigate the contact-impact force at the IRJ, the agreements of strain results are acceptable considering the explicit time integration method has certain short coming with regard to strain/stress level accuracy.